Materials Science-Poland, 33(2), 2015, pp. 230-236
http://www.materialsscience.pwr.wroc.pl/
DOI: 10.1515/msp-2015-0030

DE GRUYTER OPEN

Synthesis and photocatalytic performance of spongy ZnO microstructures

Y.L. ZOU*, Y. LI, Q. WANG, D.M. AN, X.X. LIAN, T. LV

College of Science, Civil Aviation University of China, Tianjin 300300, P. R. China

Spongy ZnO microstructures were synthesized via a facile hydrothermal method using zinc nitrate hexahydrate and oxalic acid as raw materials. The as-obtained ZnO were characterized by powder X-ray diffractometry (XRD), field emission scanning electron microscopy (FESEM), and transmission electron spectroscopy (TEM), respectively. The BET surface area and average pore size of the samples were determined by nitrogen adsorption-desorption analysis. Effects of precursor and hydrothermal temperature on the morphology and photocatalytic activity of the products were investigated. SEM and TEM analysis indicated that the as-obtained spongy ZnO microstructures consisted of a large amount of ZnO particles with the average size of about 100 to 150 nm. The photocatalytic activities of the spongy ZnO microstructures were evaluated by photodegradation of methylene blue (MB) under UV light radiation. The results indicated that the ZnO synthesized at 150 °C for 10 h showed the highest photocatalytic activity and the degradation ratio of MB reached 99.5 % for 60 min of UV light irradiation with the light intensity of 10 mW·cm^{-2}.

Keywords: *ZnO; spongy structures; hydrothermal method; microstructures*

1. Introduction

Zinc oxide (ZnO) has been considered as one of the most important semiconductor photocatalysts due to its many advantages, such as low cost, abundance, nontoxicity, physical and chemical stability, and high efficiency [1]. As is known, the properties of a material depend heavily on its structure including particle size, crystal structure, morphology, surface defects, and so on [2–7]. In order to improve the photocatalytic performance, various morphologies of ZnO photocatalysts, such as nanorods [8], nanowires [9], nanosheets [10], nanoflowers [11], have been prepared. Li et al. [8] investigated the effects of diameter size and orientation on the photocatalytic activity of ZnO and found that the photocatalytic activity of ZnO films decreased obviously with the increasing of diameter size, while the photocatalytic activity of ZnO rods was inversely proportional to diameter size. Wang et al. [6] found that ZnO nanoflowers showed higher photocatalytic activity than that of ZnO nanorods for degradation of 4-CP under UV light irradiation due to its larger specific area and the existence of more oxygen vacancies and Zn sites. Moreover, some doped ZnO microstructures with enhanced photocatalytic performance were also reported [12, 13].

Porous materials with various morphologies have attracted remarkable attention because porous materials with high porosity and specific surface area usually exhibit unique physical properties different from corresponding solid structures. Up to now, porous ZnO photocatalysts with enhanced photocatalytic activity synthesized by various methods have been reported [14–20]. Zou et al. [14] synthesized porous ZnO microspheres by a hydrothermal preparation and thermal decomposition of zinc hydroxide carbonate precursor and they pointed out that the product exhibited a significantly enhanced photocatalytic activity in comparison to commercial ZnO and TiO_2. ZnO hollow spheres, synthesized via a facile template-free aqueous solution method, showed excellent photocatalytic activity, being superior to that of commercial TiO_2 powders, for the decomposition of NOx gas under both visible-light and UV light irradiation [15]. Zheng et al. [17] prepared porous ZnO and ZnO-CTAB photocatalysts

*E-mail: zouyunling1999@126.com

by cetyltrimethylammonium bromide (CTAB) assisted sol-gel method and investigated the effect of the addition of CTAB on the photocatalytic activity of the products. They found that the ZnO-CTAB photocatalyst showed three times higher photocatalytic activity than that of the reference ZnO, and the addition of CTAB into the synthesis system not only altered the surface parameters, especially the distribution of the pores, but also enhanced the photo induced charge separation rate of ZnO. According to above references, porous ZnO photocatalysts have a broad prospect of application in photocatalysis system. Therefore, the preparation of porous ZnO photocatalyst with enhanced photocatalytic activity is still of significance.

In this study, ZnO photocatalysts with spongy microstructures were synthesized via a facile hydrothermal method using zinc nitrate hexahydrate and oxalic acid as raw materials. XRD, SEM, TEM, and BET methods were used to characterize the products. The photocatalytic activity of the spongy ZnO microstructures was evaluated by photodegradation of methylene blue (MB) under UV light irradiation. The effect of hydrothermal temperature on the morphology and photocatalytic activity of the products was also investigated.

2. Experimental

2.1. Materials

All reactants were of analytical grade and used as received without any further purification. Zinc nitrate hexahydrate ($Zn(NO_3)_2{\cdot}6H_2O$, $\geqslant$98 %), oxalic acid ($H_2C_2O_4{\cdot}2H_2O$, 99 %), and absolute ethanol (C_2H_5OH, 99.7 %) were purchased from Kewei Company of Tianjin University. Cetyltrimethylammonium bromide ($C_{19}H_{42}BrN$, CTAB) was purchased from Farco Chemical Supplies, Hong Kong. Distilled water was used throughout.

2.2. Synthesis of porous ZnO microstructures

In a typical process, 2.9749 g $Zn(NO_3)_2{\cdot}6H_2O$ was dissolved in 40 mL distilled water to form a transparent and homogeneous solution. Then, 0.2 g CTAB was added to the $Zn(NO_3)_2$ solution under vigorously stirring and kept stirring for 15 min until the adequate dissolution of CTAB. Here, CTAB was used as a surfactant, which could reduce the surface tension of the solution and make the ZnO particles have better dispersion [17]. Subsequently, 25 mL of 0.5 mol·L^{-1} $H_2C_2O_4$ solution was added drop by drop into the above solution under vigorous stirring and then the reaction solution was transferred to a 100 mL Teflon-lined stainless steel autoclave and heated at 150 °C for 10 h in an electric oven. After reaction, the autoclave was allowed to cool to room temperature. The obtained precipitate was washed thoroughly with distilled water and ethanol to neutral conditions (pH = 7), and dried at 80 °C for 24 h. Finally, the as-synthesized product was calcined in a furnace at 500 °C for 2 h under normal atmospheric conditions, and finally a white product was obtained.

2.3. Measurement and characterization

Powder X-ray diffraction (XRD) patterns were recorded on a DX-2000 X-ray diffractometer equipped with a CuKα (λ = 0.1542 nm) radiation tube operating at 40 kV and 25 mA at room temperature. A 1530VP field-emission scanning electron microscope (FESEM) was used to characterize the morphologies and sizes of the products. Transmission electron microscopy (TEM) and high-resolution TEM (HRTEM) examinations were conducted on a JEM-2010FEF transmission electron microscope (TEM) with an acceleration voltage of 200 kV. Nitrogen adsorption-desorption measurements were performed at 77 K with an Autosorb iQ-MP nitrogen adsorption apparatus (Quantachrome Instrument Corp.) utilizing the Brunauer-Emmett-Teller (BET) method in the relative pressure range of 0.05 to 0.30 for the calculation of surface areas. The sample was degassed at 200 °C for 3 h prior to nitrogen adsorption measurements. The pore size distribution was estimated from the desorption branch of the isotherm using the Barrett-Joyner-Halenda (BJH) method and the average pore size was calculated from the amount of adsorbed nitrogen at the relative pressure of 0.99.

2.4. Photocatalytic activity test

The photocatalytic activity of the spongy ZnO microstructures was evaluated by degradation of methylene blue (MB) under a UV light with a wavelength of 365 nm at room temperature (ca. 25 °C). The experimental procedure was as follows: 15 mg of the spongy ZnO powders were dispersed in 75 mL of a solution containing 10 mg·L^{-1} of MB solution under vigorous stirring in a double-wall reactor made of quartz (with a capacity of 100 mL), and cooling water was inputted between the double walls used as recycle cooling. The suspensions were placed in the dark for 30 min under vigorous stirring before illumination. The samples were taken after light irradiation for 0, 5, 10, 20, 40, 60 min, and were centrifuged with 10000 rpm for 10 min. The absorbance of the supernatant was tested at a wavelength of 665 nm by a UV-Vis spectrophotometer (T6, Beijing Purkinje General Instrument Co., Ltd). Here, a 15 mA 365 nm Xenon lamp (HXS-F/UV 300, Beijing NBet Technology Co., Ltd) was used as a light source to trigger the photocatalytic reaction, and the average light intensity striking on the surface of the reaction solution was about 10 mW·cm^{-2}. Moreover, the photocatalytic activity of Degussa P25 TiO_2 powders (P25) was also measured as a reference.

3. Results and discussions

3.1. Effect of precursor

The phase compositions and crystal structures of the precursor and the product were analyzed by XRD analysis. Fig. 1a shows the XRD pattern of the precursor obtained by hydrothermal reaction at 150 °C for 10 h in the presence of CTAB. All of the diffraction peaks can be readily indexed as zinc oxalate crystalline structure (JCPDS No. 25-1029). The XRD pattern shown in Fig. 1b was recorded for the product obtained by calcining the precursor at 500 °C for 2 h. The diffraction peaks can be clearly indexed to the hexagonal ZnO (JCPDS No. 36-1451) with cell parameters a = 3.249 Å and c = 5.206 Å. The sharp diffraction peaks reflect the excellent crystallinity of ZnO without any impurities, indicating that the precursor had completely transformed into the ZnO phase.

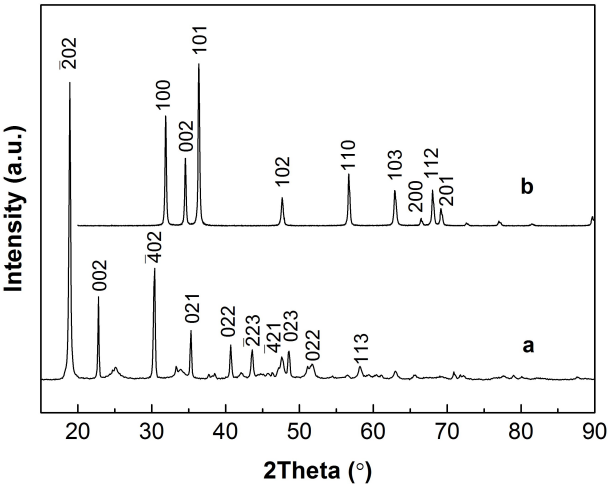

Fig. 1. XRD pattern of the precursor and the as-prepared ZnO.

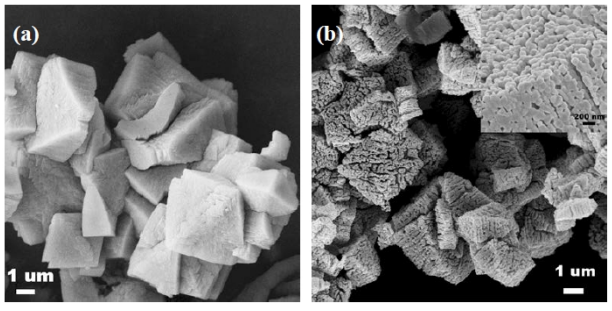

Fig. 2. SEM images of the precursor (a) and the as-prepared ZnO (b). The inset is the high-magnification image of ZnO nanostructures.

Fig. 2 shows the SEM images of the precursor synthesized by hydrothermal reaction at 150 °C for 10 h in the presence of CTAB and the corresponding product calcined at 500 °C for 2 h. It can be found from Fig. 2a that the precursor shows irregular hexahedral structure with a rough surface, the average size of which is about 3 to 5 μm. Similar structure can also be observed in the SEM image of the as-synthesized ZnO, as shown in Fig. 2b, indicating that the precursor has an important effect on the morphology of the product. Moreover, a large number of holes exist not only on the surface but also in the body of the spongy ZnO structures,

which is different to the morphology of the precursor. The porous structures can be explained in the high-magnification image of ZnO microstructures in Fig. 2b (inset), where the spongy ZnO structures are composed of large numbers of particles, with about 100 to 150 nm in diameter, which are stacked together to form the porous structure.

TEM images have been used to investigate the structure of the spongy ZnO microstructures in detail. As shown in Fig. 3a, the spongy ZnO microstructures consist of large numbers of particles and have porous structure. This result is consistent with the SEM result (Fig. 2b, inset). Fig. 3b shows the high resolution TEM images of the spongy ZnO microstructures, where clear lattice fringes can be observed. The lattice spacings of 0.286 nm and 0.289 nm between adjacent lattice planes correspond to the crystal plane of (100).

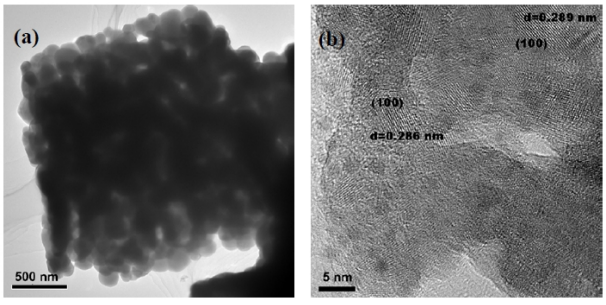

Fig. 3. TEM (a) and HRTEM (b) images of the as-prepared ZnO.

3.2. Effect of hydrothermal temperature

In order to investigate the effect of hydrothermal temperature on the phase structure and morphology of the products, a series of samples were prepared at different hydrothermal temperatures. Fig. 4 shows the X-ray diffraction patterns and SEM images of the products. It can be found from Fig. 4a that all the peaks are in good agreement with the hexagonal wurtzite structure of ZnO (JCPDS No. 36-1451). This result reveals that hydrothermal temperature has no effect on phase structure of the product. Fig. 4b, 4c and 4d show the SEM images of the spongy ZnO prepared at 120 °C, 150 °C, and 180 °C, respectively. It can be found that the particle size of the products increases slowly with the increase of hydrothermal temperature. Though the particles size of the ZnO prepared at 120 °C is small, it is less uniform compared with that of the ZnO prepared at 150 °C and 180 °C. Particle aggregation can be observed in Fig. 4d, indicating that much higher hydrothermal temperature would lead to the aggregation of the particles.

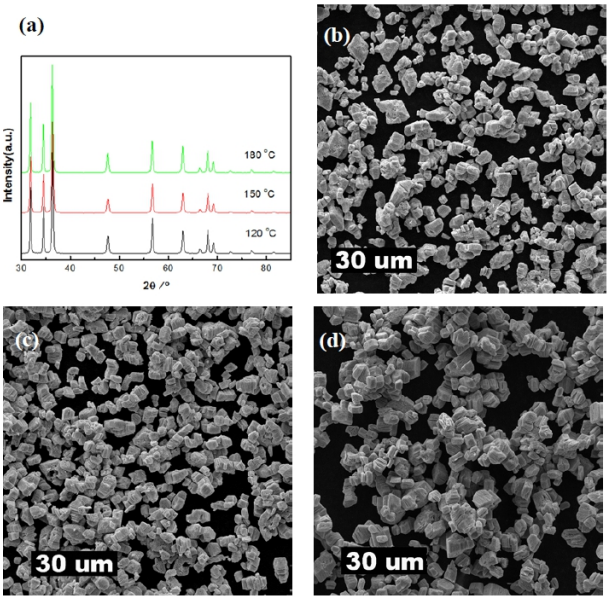

Fig. 4. XRD patterns (a) and SEM images of the ZnO prepared at different hydrothermal temperatures: (b) 120 °C; (c) 150 °C; (d) 180 °C.

3.3. BET analysis

The nitrogen adsorption-desorption analyzed by the Brunauer-Emmett-Teller (BET) method was employed to study the surface properties of the spongy ZnO microstructures prepared at 150 °C for 10 h, as shown in Fig. 5. The isotherm of the spongy ZnO exhibits type-IV curve. At high relative pressure range between 0.8 and 1.0, the curve exhibits a clear hysteresis loop indicating the presence of mesopores. The spongy ZnO shows a specific surface area of 15.0 m^2/g. The pore size distribution in the sample, studied also using the BJH method as shown in Fig. 5 (inset), shows two peaks in the range of 1 to 15 nm at 1.9 and 7.8 nm. This result indicates that the spongy ZnO show hierarchically porous structures. According to Yu

et al. [21], N_2 adsorption-desorption analyses cannot provide macroporous information of the sample. Therefore, the macroporous structure of the spongy ZnO microstructures can be observed in the SEM image (Fig. 2b) and TEM image (Fig. 3a).

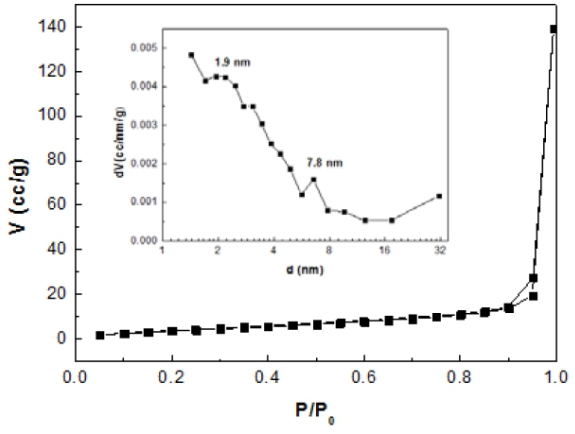

Fig. 5. N_2 adsorption-desorption isotherms of the spongy ZnO microstructures prepared at 150 °C for 10 h. The inset indicates the pore size distribution of the ZnO, calculated from the desorption branch by the BJH model.

3.4. Formation mechanism of spongy ZnO microstructures

Sponge-like macro-/mesoporous materials with enhanced performance have been widely reported in recent years [21, 22]. Yu et al. [21] prepared trimodally sponge-like macro-/mesoporous titania by hydrothermal treatment of precipitates of tetrabutyl titanate ($Ti(OC_4H_9)_4$) in pure water and they concluded that the formation of the sponge-like macro-/mesoporous structures was the result of the cooperative effect of hydrodynamic flow of water, and restructuring and phase transformation of amorphous TiO_2 during hydrothermal treatment. Chen et al. [22] synthesized spongy CuO via direct pyrolysis of $Cu_3(btc)_2$ (btc = benzene-1,3,5-tricarboxylate) microporous metal-organic framework (MOF) in the air, using $Cu_3(btc)_2$ as the Cu source and complexing molecule precursor. They found that the formation of CuO was induced by the decomposition of inorganic-organic hybrid materials related to the btc and copper ions. In our experiments, spongy ZnO microstructures were synthesized by hydrothermal method using zinc nitrate hexahydrate and oxalic acid as raw materials, and CTAB as a surfactant. On the basis of the obtained XRD as well as nitrogen adsorption, SEM, and TEM investigation results, a possible formation mechanism of spongy ZnO microstructures can be proposed. When $H_2C_2O_4$ solution was dropped into the $Zn(NO_3)_2$ solution containing CTAB, Zn^{2+} reacted with oxalic acid first to form a water-soluble complexes due to the existence of CTAB. After hydrothermal treatment at 150 °C for 10 h, zinc oxalate formed a precursor (as shown in Fig. 1a). Spongy ZnO microstructures, which showed similar structure to the precursor, were obtained by calcination of the precursor at 500 °C for 2 h. The meso/macro-pores derived from the decomposition of zinc oxalate due to formation of CO_2, can be observed in Fig. 2b and Fig. 3a. Therefore, it can be concluded that the precursor has an important effect on the morphology of the product. Of course, the detailed formation mechanism on hierarchically spongy structures needs to be further investigated in our future work.

3.5. Photocatalytic measurements

Methylene blue (MB), a widely used dye, was selected as the model pollutant to evaluate the photocatalytic activities of P25 and the spongy ZnO microstructures prepared at different hydrothermal

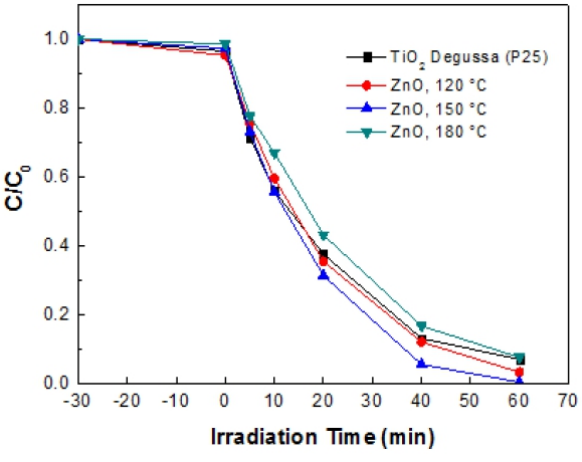

Fig. 6. MB concentration changes over P25 and spongy ZnO microstructures.

temperatures. Fig. 6 shows the relationship between the concentration ratio of MB (C/C_0) and radiation time, where C is the concentration of MB solution at time t, and C_0 is the concentration of MB solution at the beginning. After 30 min of dark adsorption, the amounts of MB remaining in the solution containing ZnO powders prepared at 120 °C, 150 °C, and 180 °C, are 95.3 %, 97.4 %, and 98.6 %, respectively. The concentrations of MB decrease rapidly with an increase in UV illumination time, indicating that all the ZnO powders show excellent photocatalytic activities. The concentration of MB in the solution containing the ZnO powder prepared at 150 °C for 10 h is close to 0 after 60 min of UV light irradiation with the light intensity of 10 $mW \cdot cm^{-2}$, demonstrating that this product shows the highest photocatalytic activity. Comparing the morphology of three samples (shown in Fig. 4b, 4c, 4d), it can be found that the ZnO powders synthesized at 150 °C have a relatively small diameter size as well as good dispersibility. Therefore, it can be inferred that both diameter size and dispersibility have important influences on the photocatalytic activity of the ZnO powders. Form Fig. 6 it can also be found that the photocatalytic activities of the ZnO powder synthesized at 120 °C and 150 °C for 10 h are higher than that of P25. It can be explained by the unusual hierarchically porous structure of the ZnO microstructures, which allows more efficient transport for the reactant molecules to get to the active sites on the framework walls [19]. According to the references [23–25], ·OH radicals, which have been generated by oxidation of surface water by the holes, are responsible for many oxidation pathways of chemical compounds initiated through heterogeneous photocatalytic processes. In our experiments, the amount of oxygen vacancy defects on the ZnO surface synthesized at 150 °C was higher than in the other two samples synthesized at 120 °C and 180 °C, confirming the best photocatalytic performance of the ZnO powder synthesized at 150 °C. Moreover, the amount of photocatalyst also had a significant effect on the photocatalytic activity of ZnO [7, 26, 27]. The research results showed that when the amount of photocatalyst did not exceed a certain critical value, photocatalytic efficiency would increase with the increasing of photocatalyst amount. In our case, the photocatalyst amount of ZnO with small BET surface area (Fig. 5a), is relatively small (0.2 g/L), while the degradation ratio of MB reaches 99.5 % for 60 min of UV light radiation. Therefore, the spongy ZnO microstructures can become an excellent photocatalyst, the photocatalytic activity of which can be further improved by increasing their BET surface area.

4. Conclusions

In this paper, we have synthesized ZnO microstructures by hydrothermal method and investigated their photocatalytic activity by degrading 10 $mg \cdot L^{-1}$ MB using a UV light with a wavelength of 365 nm. Experimental results show that the as-prepared ZnO are made of spongy microstructures, which consist of a large amount of ZnO particles with the average size of about 100 to 150 nm. The spongy ZnO structures show high photocatalytic activity to methylene blue (MB) under UV light radiation with the light intensity of 10 $mW \cdot cm^{-2}$. The spongy ZnO prepared at the hydrothermal temperature of 150 °C shows the highest photocatalytic activity (degradation ratio of MB, nearly 100 % for 60 min of UV light radiation).

Acknowledgements

The work was supported by the Significant Pre-research Funds of Civil Aviation University of China (3122013P001), the Science and Technology Innovation Guide Funds of Civil Aviation Administration of China (2014), and the Fundamental Research Funds for the Central Universities (3122014K016).

References

[1] Daneshvar N., Salari D., Khataee A.R., *J. Photoch. Photobio. A*, 162 (2004), 317
[2] Chen D.M., Wang Z.H., Ren T.Z., Ding H., Yao W.Q., Zong R.L., Zhu Y.F., *J. Phys. Chem. C*, 118 (2014), 15300.
[3] Han Z.Z., Liao L., Wu Y.T., Pan H.B., Shen S.F., Chen J.Z., *J. Hazard. Mater.*, 217 – 218 (2012), 100.
[4] Kim D., Huh Y.D., *Mater. Lett.*, 65 (2011), 2100.
[5] Gupta J., Bhargava P., Bahadur D., *Physica B*, 448 (2014), 19.
[6] Wang Y.X., Li X.Y., Wang N., Quan X., Chen Y.Y., *Sep. Purif. Technol.*, 62 (2008), 732.

[7] LI G.Q., Y Z.G., WANG H.T., JIA C.H., ZHANG W.F., *Appl. Catal. B-Environ.*, 158 – 159 (2014), 280.
[8] LI X.Y., WANG J., YANG J.H., LANG J.H., LÜ S.Q., WEI M.B., MENG X.W., KOU C.L., LI X.F., *J. Alloy. Compd.*, 580 (2013), 205.
[9] CHANG J.H., LIN H.N., *Mater. Lett.*, 132 (2014), 134.
[10] KAEWMARAYA T., DE SARKAR A., SA B., SUN Z., AHUJA R., *Comp. Mater. Sci.*, 91 (2014), 38.
[11] ADHYAPAK P.V., MESHRAM S.P., AMALNERKAR D.P., MULLAN I.S., *Ceram. Int.*, 40 (2014), 1951.
[12] LV W., WEI B., XU L.L., ZHAO Y., GAO H., LIU J., *Appl. Surf. Sci.*, 259 (2012), 557.
[13] LIANG G.F., HU L.W., FENG W.P., LI G.D., JING A.H., *Appl. Surf. Sci.*, 296 (2014), 158.
[14] LEI A.H., QU B.H., ZHOU W.C., WANG Y.G., ZHANG Q.L., ZOU B.S., *Mater. Lett.*, 66 (2012), 72.
[15] WEI Y.L., HUANG Y.F., WU J.H., WANG M., GUO C.S., DONG Q., YIN S., SATO T., *J. Hazard. Mater.*, 248 – 249 (2013), 202.
[16] LI Q., LIU E.T., LU Z., YANG H., CHEN R., *Mater. Lett.*, 130 (2014), 115.
[17] ZHONG J.B., LI J.Z., XIAO Z.H., HU W., ZHOU X.B., ZHENG X.W., *Mater. Lett.*, 91 (2013), 301.
[18] ZHOU M., LV W., LIU C.L., LIU D.M., WANG Y.P., *J. Mater. Sci.-Mater. El.*, 24 (2013), 36.
[19] YU J.G., YU X.X., *Environ. Sci. Technol.*, 42 (2008), 4902.
[20] LAN S., LIU L., LI R.H., LENG Z.H., GAN S.C., *Ind. Eng. Chem. Res.*, 53 (2014), 3131.
[21] YU J.G., ZHANG L.J., CHENG B., SU Y.R., *J. Phys. Chem. C*, 111 (2007), 10582.
[22] CHEN L.Y., ZHAO C.L., WEI Z.D., WANG S.N., GU Y., *Mater. Lett.*, 65 (2011), 446.
[23] ISHIBASHI K., FUJISHIMA A., WATANABE T., HASHIMOTO K., *Electrochem. Commun.*, 2 (2000) 207.
[24] XIAO Q., SI Z.C., ZHANG J., XIAO C., TAN X.K., *J. Hazard. Mater.*, 150 (2008) 62.
[25] XIANG Q.J., YU J.G., WONG P.K., *J. Colloid Interf. Sci.*, 357 (2011) 163.
[26] SUN L., AN T.C., WAN S.G., LI G.Y., BAO N.Z., HU X.H., FU J., SHENG G.Y., *Sep. Purif. Technol.*, 68 (2009), 83.
[27] YANG L.Y., DONG S.Y., SUN J.H., FENG J.L., WU Q.H., SUN S.P., *J. Hazard. Mater.*, 179 (2010), 438.

Received 2014-10-22
Accepted 2014-12-12